Physica Medica 30 (2014) 888–897

Contents lists available at ScienceDirect

Physica Medica

journal homepage: http://www.physicamedica.com

Original paper

Exploring Boron Neutron Capture Therapy for non-small cell lung cancer

Rubén O. Farías [a, b], Silva Bortolussi [c, d], Pablo R. Menéndez [e], Sara J. González [a, b, *]

[a] Comisión Nacional de Energía Atómica (CNEA), Av. Gral. Paz 1499, Buenos Aires B1650KNA, Argentina
[b] Consejo Nacional de Investigaciones Científicas y Técnicas (CONICET), Av. Rivadavia 1917, Buenos Aires C1033AAJ, Argentina
[c] Department of Physics, University of Pavia, via Bassi 6, Pavia 27100, Italy
[d] National Institute of Nuclear Physics (INFN), via Bassi 6, Pavia 27100, Italy
[e] Insituto de Oncología "Angel H. Roffo", Universidad de Buenos Aires, Av. San Martin, n° 5421, Buenos Aires C1417DTB, Argentina

ARTICLE INFO

Article history:
Received 16 April 2014
Received in revised form
2 July 2014
Accepted 30 July 2014
Available online 28 August 2014

Keywords:
BNCT
Lung tumours
Tumour control probability
MCNP

ABSTRACT

Boron Neutron Capture Therapy (BNCT) is a radiotherapy that combines biological targeting and high LET radiation. It consists in the enrichment of tumour with ^{10}B and in the successive irradiation of the target with low energy neutrons producing charged particles that mainly cause non-repairable damages to the cells.

The feasibility to treat Non Small Cells Lung Cancer (NSCLC) with BNCT was explored. This paper proposes a new approach to determine treatment plans, introducing the possibility to choose the irradiation start and duration to maximize the tumour dose. A Tumour Control Probability (TCP) suited for lung BNCT as well as other high dose radiotherapy schemes was also introduced.

Treatment plans were evaluated in localized and disseminated lung tumours. Semi-ideal and real energy spectra beams were employed to assess the best energy range and the performance of non-tailored neutron sources for lung tumour treatments.

The optimal neutron energy is within [500 eV–3 keV], lower than the 10 keV suggested for the treatment of deep-seated tumours in the brain. TCPs higher than 0.6 and up to 0.95 are obtained for all cases.

Conclusions drawn from [Suzuki et al., Int Canc Conf J 1 (4) (2012) 235–238] supporting the feasibility of BNCT for shallow lung tumours are confirmed, however discussions favouring the treatment of deeper lesions and disseminated disease are also opened. Since BNCT gives the possibility to deliver a safe and potentially effective treatment for NSCLC, it can be considered a suitable alternative for patients with few or no treatment options.

Introduction

Boron Neutron Capture Therapy (BNCT) is a binary form of experimental radiotherapy based on the administration of a drug able to concentrate ^{10}B in the tumour more than in healthy tissues, and on the successive irradiation of the target with low energy neutrons [1]. The exploited reaction is the neutron capture in ^{10}B, which has a cross section of 3837 b at thermal energies. The neutron capture gives rise to high LET radiation, generating an alpha particle and a ^{7}Li nucleus with ranges in tissues comparable to a cell diameter. As the energy deposition is spatially confined in the cells where neutrons are captured, dose delivery is selective at a cellular level without requiring the irradiation field to tightly match the shape of the target. This characteristic makes BNCT a potential option for tumours that cannot be surgically removed nor treated with a fractionated photon-therapy or stereotactic ablative body radiation therapy (SABR) protocol because of their location, stage or patient overall status.

The tumours affecting lungs are one of the most common causes of death for cancer in the world. Given that BNCT combines biological targeting and high LET radiation, its application to lung malignancies would offer the following advantages:

a. The possibility of delivering a hypofractioned or even a single-fraction treatment.
b. The ability to treat micrometastatic or diffuse disease.

* Corresponding author. Comisión Nacional de Energía Atómica (CNEA), Av. Gral. Paz 1499, Buenos Aires B1650KNA, Argentina.
E-mail addresses: srgonzal@gmail.com, srgonzal@cnea.gov.ar (S.J. González).

http://dx.doi.org/10.1016/j.ejmp.2014.07.342
1120-1797/

c. To disregard those complex techniques that manage the respiratory motion during conventional external radiotherapy, because the cell damage depends on the boron localization.

A preclinical study to assess normal lung tolerance to BNCT was performed in small animals at MIT (USA) with the aim to understand the human lung toxicity observed during cranial treatments [2].In Japan, preclinical studies demonstrated that BNCT was feasible for malignant pleural mesothelioma (MPM) and between 2008 and 2012 patients affected by MPM were treated using epithermal neutron beams, without causing toxicity to the healthy lung and the other involved tissues [3].

At University of Pavia (Italy), a study of BNCT for pulmonary metastases form colon adenocarcinoma is ongoing. Boronophenylalanine biodistribution studies in a rat model showed that the ratios between the boron concentration in tumour and in normal lung are suitable for a safe and effective treatment [4]. These results were recently complemented by those of Trivillin et al. [5], showing that absolute boron concentration values in lung metastases are therapeutically useful either for protocols employing BPA or decahydrodecaborate (GB-10) alone or in combination. Within the context of the treatment of non-surgically resectable lung metastases, biodistribution and radiotolerance BNCT studies in a normal lung sheep model are being also carried out considering an explanted organ irradiation protocol.[1]

The present paper presents the results of the analysis of different BNCT irradiation protocols for some clinical scenarios of lung cancer. The evaluation of the potential application of BNCT has been extended to non-small cell lung cancer (NSCLC), a tumour that showed good response to hypofractionated, high dose radiotherapy schemes (i.e. SABR). The selected cases, however, were not eligible for this therapy because of the tumour proximity to critical organs at risk. These cases are: a localized early stage NSCLC in the upper side close to the costal wall, a deep localized early stage NSCLC tumour located close to the trachea and proximal bronqui, and a theoretical case of oligometastatic disease encompassing the whole lung volume.

Semi-ideal epithermal neutron sources from 100 eV to 6 keV were evaluated to give indications about the optimal characteristics of the neutron source conceived for lung BNCT. Moreover, the spectra of two constructed or projected neutron beams tailored for brain tumours were tested.

One novelty of our approach is to determine the optimum start time and duration of the irradiation using the boron concentration–time profiles in healthy lung and in tumour. In order to evaluate the potential effectiveness of the proposed treatments a suitable tumour control probability model for the treatment of NSCLC with BNCT has also been introduced and validated.

Based on the application of the mentioned radiobiological model and following currently used clinical SABR criteria and experience, some treatment plans delivered in a single BNCT session were assessed and those most promising were thoroughly discussed.

Materials and methods

Different clinical scenarios were taken into account in order to explore the possibility to treat with BNCT a wide range of patients who would have few possibilities with the current clinical options. In the following subsections, the computational and theoretical models introduced in this work are presented in detail, and the evaluation criteria to assess candidate plans are finally described.

[1] Ongoing lung autotransplant study in sheep.

The thorax model

The computational tool used to create the anthropomorphic model of the patients and to analyse the results of the irradiation simulations is a beta version of the Treatment Planning System developed in Argentina. By means of the optimized geometrical reconstruction method called MultiCell, an accurate volumetric model can be generated from the patient CT images by combination of multiple-sized parallelepiped cells suitable for MCNP code [6]. In this way, the total number of cells can be kept relatively low, while ensuring a high precision in the reconstruction. Figure 1 shows an example of a MultiCell reconstruction of a human thorax that evidences the use of different sized cells.

Anthropomorphic models were segmented in the relevant tissues with atomic composition and density taken from ICRU 46 report [7]. Volumes of interest are automatically coded into MCNP.

A superimposed mesh grid of 125 mm^3 is used to calculate the different dose components and a subsequent interpolation is performed to assign the dose values to each pixel of the images. The results are then properly weighted and summed to calculate the total dose.

The neutron sources

The epithermal beams designed for the treatment of deep-seated tumours have energies centred around 10 keV [8]. However, as high energy neutrons deliver higher doses in the first layers of tissues, organ such as the skin and the spinal cord may limit the dose administered to the tumour in case of thorax irradiation.

In this work, several semi-ideal neutron beams were tested on the human thorax models in order to explore advantages and drawbacks related to the extensive irradiation of NSCLC with neutrons. The energy of these sources was sampled from Gaussian distributions with mean energies of 100 eV, 500 eV, 1 keV, 3 keV and 6 keV, and standard deviations of 0.02 keV for mean energies up to 1 keV, and 0.2 keV for the others.

Based on the conclusions drawn from the aforementioned semi-ideal beams, two realistic neutron spectra from existing or projected BNCT facilities were selected from literature and evaluated. The first realistic beam, named MIT-SPECT, is based on the published energy spectrum of the MIT-II epithermal reactor beam developed for BNCT [9]. The beam spectrum is characterized by 95% of the neutrons in the [0, 10 keV] energy range, and approximate 20% between 500 eV and 3 keV. The second realistic beam, named CNEA-MEC, is based on one of the energy spectra published by Capoulat et al. [10]. for an accelerator based epithermal neutron beam that is being designed in Argentina to treat deep-seated GBM tumours with BNCT. In this case, 90% of the neutrons are between 0.2 eV and 20 keV, and almost 30% in the [500 eV–3 keV] energy range. The spectrum of these realistic neutron beams are presented in Fig. 2. Sources particles were sampled uniformly in a plane and particle direction set monodirectional normal to that plane.

Simulations for both semi-ideal and realistic beams were carried out normalizing their corresponding thermal neutron flux peaks in water to 5×10^9 n cm^{-2} s^{-1}. Particle transport was performed without explicitly considering the unavoidable gamma contamination of the beam. However, the contribution of this radiation component to the total dose was taken into account by increasing 50% the induced gamma dose in tissues from H and B.

For localized NSCLC, the beam was set circular with a 10 cm diameter. For multiple metastatic NSCLC the source diameter was increased to 20 cm in order to encompass the lung volume completely. If necessary, a 30 mm thick boronated polyethylene frame was added to the port to reduce the port free area and to

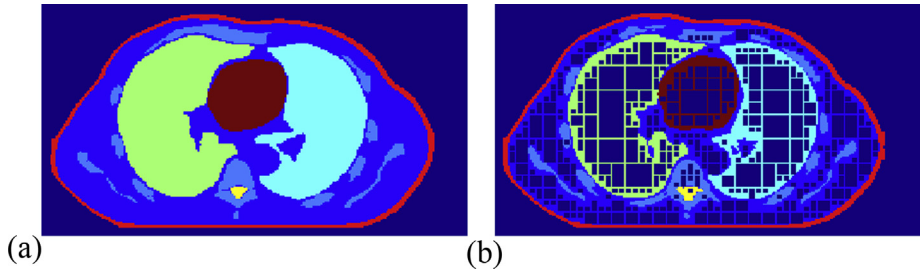

Figure 1. (a) Volumes of Interest marked for reconstruction in a coronal view of the human thorax, and (b) corresponding MultiCell-based model for MCNP. Cell dimensions vary according to the spatial distribution of the materials, thus ensuring a high precision in the geometrical representation as well as a relatively small number of cells.

spare the surrounding normal tissue, especially skin and superficial soft tissues.

Dose calculations

The component of the BNCT dose due to ionizing charged particles comes from neutron capture reactions in ^{10}B and in ^{14}N, neutron scattering in ^{1}H, and (both induced and structural) gamma interactions with matter, which release respectively α, ^{7}Li, protons and primary electrons in tissues. Charged particle equilibrium is assumed everywhere in the medium and each dose contribution is calculated using the MCNP tally f4 (fluence tally) coupled to neutron kerma factor and X-ray mass attenuation coefficient tables. For the boron component, the kerma factor table for 1 ppm concentration reported in Ref. [11] was employed. The gamma component was calculated with the X-ray mass attenuation coefficients table reported in Ref. [12]. The dose component due to neutrons (thermal capture in nitrogen and epithermal scattering on hydrogen) was calculated using the lung kerma factors from ICRU 63 [7] and cross sections and Q values from JENDL-3.2 [13]. The use of lung kerma factors to compute doses in all the organs of interest guarantees to obtain accurate values in the lung and good estimates of the doses in the remaining organs.

Photon-equivalent doses (Gy_w) were computed by multiplying each absorbed dose component by the Relative Biological Effectiveness (RBE) factor and the Compound Biological Effectiveness (CBE) factor reported in Table 1. CBE factors were evaluated in the case of healthy lung and the boron carrier BPA at MIT [14]. In this work, the weighting factor corresponding to the early breathing rate increase has been taken into account because an acute toxicity would be the most immediate concern in case of NSCLC patients. For the skin and tumour tissues, factors taken from the literature were used [15,16]. Remaining normal tissues factors are the same as lung tissue following BNCT clinical experience in other treatment locations [16].

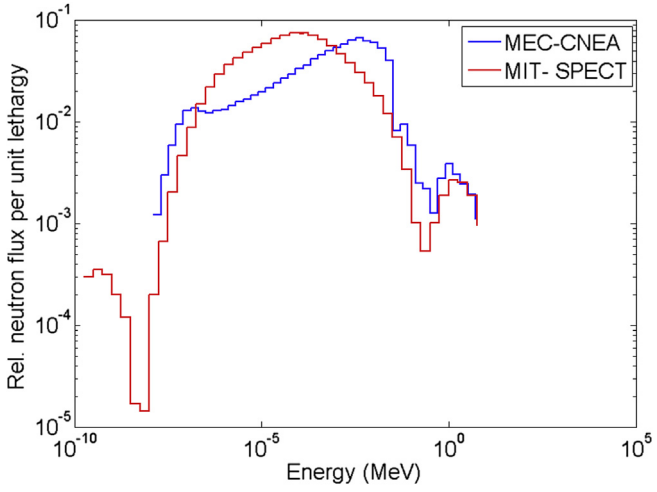

Figure 2. Relative neutron flux per unit of lethargy as function of energy for the beams MIT-SPECT and CNEA-MEC based on epithermal reactor and accelerator based neutron sources.

BPA kinetics considerations

The dose calculation requires the knowledge of the boron concentration present in each tissue involved in the irradiation. In Pavia, a pharmacokinetic study was performed using a rat model bearing diffuse lung metastases from colon carcinoma. The rats were injected with BPA, 300 mg/kg b.w., and sacrificed after different intervals of time. The boron concentration was then measured in samples of normal lung and tumour by spectrometry and neutron autoradiography [4].

Based on this pharmacokinetic study, the average behaviour of BPA in normal lung and tumour tissues as a function of time was obtained by fitting rescaled measured data with an open two compartment model (Fig. 3a) [17]. Biodistribution studies in big animals and humans using the same dose of BPA revealed that: a) the boron uptake in healthy lung is the same as the concentration in blood, and b) boron average values in blood 60 min after the end of infusion are around 20 ppm. Then, this information was used to calculate the "animal-to-human rescaling factor" to fulfil point b). Boron concentration in patients was assumed to be the same in all the normal tissues of interest (healthy lung, heart, spine, soft tissue and ribs) as adopted in all BNCT clinical trials. For the skin, a tissue-to-normal lung boron concentration ratio of 1.5 was applied [15].

The pharmacokinetic curves were employed to determine the optimum irradiation scenario for each analysed clinical case. According to the dose limitations imposed by the radiosensitivity of the different organs, the optimal start time and duration of the irradiation were obtained by maximizing the minimum dose in the tumour.

Figure 3b depicts the 1.5 h averaged tumour-to-normal tissue boron concentration ratio as a function of the irradiation start time. Since the proposed treatments are not short enough to consider the tumour-to-normal ratio constant during the irradiation, the time-

Table 1
RBE and CBE factors used to convert the absorbed dose (Gy) into photon equivalent dose (Gy_w).

BNCT dose component	Normal tissues	Tumour	Skin
10B(n,α)7Li	1.4	3.8	2.5
14N(n,p)14C	3.2	3.2	3.2
Fast neutron	3.2	3.2	3.2
Photons	1	1	1

Endpoint: early breathing rate increase.

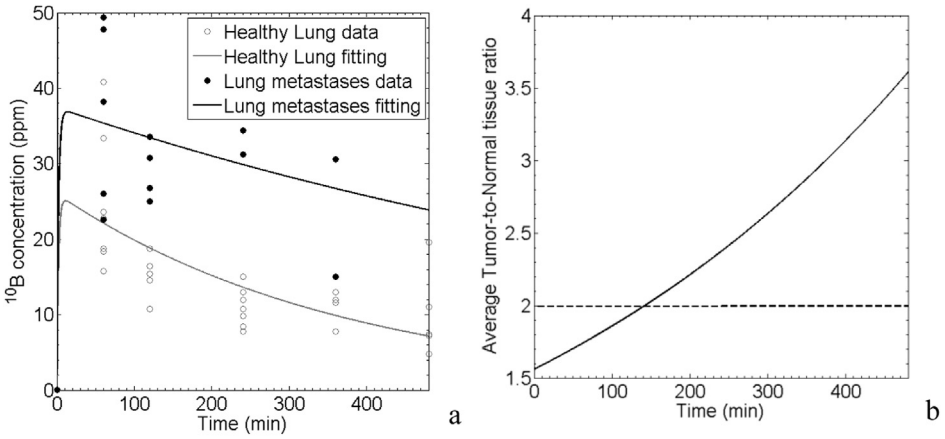

Figure 3. (a) 10B concentration–time profiles with the fit using the open two compartments model for healthy lung and pulmonary metastasis. Profiles are plotted as a function of the time after BPA administration. Open circles: Rescaled healthy lung experimental data; filled circles: Rescaled lung metastases experimental data; gray line: fit of the experimental healthy lung concentrations; black line: fit of the experimental concentrations in metastases. (b) 1.5 h Averaged tumour-to-normal tissue boron concentration ratio plotted as a function of the infusion start time. The horizontal dashed line represents the minimum ratio for patient eligibility in Suzuki et al. [18].

averaged value is a more realistic estimate of the expected ratio during the treatment.

Typically, a tumour-to-normal tissue ratio of 2 or greater is considered suitable for patient eligibility in BNCT protocols, even if a 3.5 ratio is taken as the reference for the dosimetry calculations [19]. Note that from 150 min after infusion start in Fig. 3b the ratio satisfies the eligibility criteria.

Extending a suitable tumour control probability model for the treatment of NSCLC with BNCT

An extension of a tumour control probability model for non-uniform dose distributions has been introduced and employed to evaluate the treatments outcome. The proposed model essentially exploits the general form for the TCP of an inhomogeneously irradiated tumour presented in Ref. [20] and the corresponding model parameters derived from the retrospective analysis of 66 patients of NSCLC treated with curative intent. Details of the model can be found in Appendix A.

Dose prescription and evaluation criteria

Dose Volume Histograms (DVH) for each organ (or Volume of Interest, VOI), and isodose curves were used to analyse the different tested treatment plans in all the cases. Common criteria chosen to evaluate the treatment plans were taken from the National Comprehensive Cancer Network (NCCN) guidelines for Non-small cell lung cancer [21], Timmerman et al. [22], and AAPM task group no. 101 report on SABR for lung cancer [23].

The constraints adopted to accept a treatment plan were:

1. Heart $D_{max} < 22$ Gy
2. Spinal cord $D_{max} < 14$ Gy
3. Skin $V_{23Gy} < 10$ cc or $D_{max} < 26.0$ Gy
4. Oesophagus $D_{max} < 15.4$ Gy
5. Trachea & proximal Bronchi $D_{max} < 20.2$ Gy
6. Ribs $D_{max} < 30$ Gy

Localized tumour

In the case of localized tumour, the healthy lung is defined as the total left and right disease-free lung volume, and the adopted constraints are:

1. More than 1500 cc with a dose below 7 Gy to assure basic lung function or, more than 1000 cc with a dose below 7.4 Gy to 20% pneumonitis probability and,
2. $V_{20Gy} < 10\%$.

In these cases, Planning Target Volume (PTV) was considered as the Clinical Target Volume (CTV) plus a safety margin up to 30 mm in all directions, according with the CTV location and motion.

Dose prescription was decided based on SABR single fraction experience [24]. A dose of 30 Gy_W or more to the PTV was prescribed in a single fraction, whenever possible without exceeding the OAR constraints. If this criterion could not be fulfilled, the second goal was to maximize the dose to the PTV in order to assure the highest theoretical TCP.

Conformity index evaluation for localized lung tumours in BNCT. One of the main goals of SABR is to ensure a steep dose gradient between PTV and surrounding normal tissues. In order to quantify the dose falloff the Conformity Index (CI) is used. CI_x is defined as the ratio of total patient volume encompassed by X% isodose line and the PTV volume receiving the same dose. BNCT dose distribution is characterized by steep falloffs between different tissues depending on boron uptake. The application of this concept to BNCT as it is defined hides the real falloff existing between PTV and healthy lung. Thus, we defined the Lung Conformity Index (LCI_x) as the ratio between the volume of the main organ at risk encompassed by X% isodose line and the PTV volume receiving the reference dose.

Comparison of both LCIs and CIs versus SABR data reported in Ref. [25] was performed, adopting the same reference dose criterion: the 80% isodose was assigned to the dose encompassing 95% of PTV volume.

Oligometastatic pulmonary disease

Following Hellman and Weichselbaum criteria [26]patients affected by 1–5 pulmonary nodules, with good performance status and absent or stable extrathoracic disease are considered. Van Dyk reported 7.5 Gy mid-lung dose as a safe value for whole lung irradiation (WLI) in order to avoid radiation pneumonitis [27]. Considering this result and that the location of the lesions are assumed unknown, prescription was set to 7.5 Gy (mean dose) to whole lung and PTV was defined to coincide with the entire lung volume (i.e., similar to WLI criteria).

Results

In the following, the outcomes for each clinical case are presented. Two real cases of localized tumours are analysed, one shallow and another deep-seated, and an ideal case of disseminated metastases.

Localized early stage NSCLC

Case 1: shallow localized NSCLC

The first case is a patient with shallow localized NSCLC (T2N0M0) treated in real life by fractionated 3DC-RT.

Considering ^{10}B biological selectivity and CTV location, the radio-oncologist selected a PTV safety margin of 20 mm in all directions for this case. This margin is more similar to those contoured in 3DC-RT rather than the recommended margins in SABR. As in BNCT there is no breath motion control, our selection ensures complete target coverage during normal breath motion while sparing the healthy lung due to the preferential accumulation of the boron compound in tissues.

Several treatment configurations were tested starting with 5 portals distributed around the PTV isocenter point, as shown in Fig. 4. Both for semi-ideal and realistic neutron beams the best dosimetric outcomes were obtained with 3 beam incidences (Posterior, Left Anterior Oblique, Right Anterior Oblique) configuration. Portal weights were adjusted for each configuration.

Partial results of case 1. Treatments with semi-ideal beams allow delivering the prescription dose to the PTV (i.e, a minimum dose of 30 Gy_W) in total irradiation times from 88 to 96 min, comparable to current clinical applications of BNCT. The treatment starts around 7 h after BPA infusion. For these conditions, average boron concentration values of 7.8 ppm and 24 ppm are obtained in normal lung and tumour tissues, respectively. These values correspond to the typical tumour-to-healthy lung ^{10}B ratio of about 3. The doses absorbed by the organs at risk, except from the skin, remain 10%–50% lower than the safety constraints. Particularly, the healthy lung volume receiving less than 7 Gy_W is larger than 2100 cc in all the cases, results that are dosimetrically promising to expect low radiotoxic effect in this organ after irradiation.

As shown in Fig. 5, skin overdose is observed for the treatments with 100 eV and 6 keV beams, while the maximum skin dose is below the constraint (26 Gy) for 500 eV, 1 keV and 3 keV beams.

In addition, the PTV dose homogeneity increases with beam energy. However, the healthy lung volume receiving a dose higher than 7.4 Gy_W reaches a minimum with 3 keV beam.

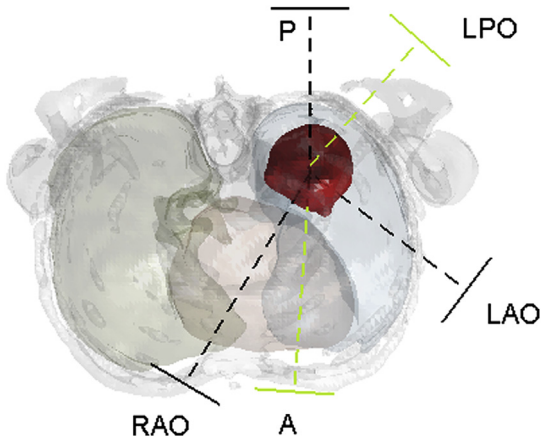

Figure 4. Complete set of portal incidences tested in case 1. Highlighted darker dashed lines are those portals corresponding to the best configuration obtained.

Theoretical tumour control probabilities were calculated for 500 eV, 1 keV and 3 keV beams, the ones that proved suitable regarding all dose constraints. TCP values close to 0.96 were obtained for all cases. In fact both mean and maximum doses are well above the PTV prescription dose, increasing from 35 Gy_W to 40 Gy_W and 58 Gy_W to 62 Gy_W, respectively, as beam energy increases (Fig. 6).

These results indicate that an "ideal" beam for the analysed treatment would be essentially epithermal, with a primary energy between 500 eV and 3 keV and with low neutron contributions for energies outside 500 eV – 3 keV range. Realistic neutron beams have broader energy spectra with non-desirable neutron contributions outside the mentioned range, thus the application of these beams would affect the treatment planning and the optimum results obtained with ideal beams. To quantify this effect, a number of treatment plans were assessed using the MIT-SPECT and MEC-CNEA sources, beams that have spectral characteristic similar to the ones assessed above. A 30 Gy_W minimum PTV dose prescription was adopted as before, as well as the treatment time windows optimization algorithm based on boron biodistribution profiles. The best treatment plans achieved under mentioned conditions guarantee that all the organ at risk except the skin receive doses below safety limits, within the range observed for semi-ideal beams. However, skin doses exceeding 26 Gy_W are obtained in volumes of about 50 cc (6%), due to the contribution of the fast component of the realistic beam spectra.

The second prescription criterion was then applied to maximize the PTV minimum dose without exceeding safety dose levels. This resulted in PTV minimum doses of about 20 Gy_W. Time windows optimization algorithm was applied in order to maximize the ratio between mean healthy lung dose and the PTV minimum dose. For both the beams the irradiation start time was 5 h after infusion, with a total duration 30 min shorter than that necessary for semi-ideal beams (i.e., around 60 min). Compared to the values obtained for semi-ideal beams, the concentration in healthy lung is higher in this case and the average tumour-to-normal tissue ratio decreased to 2.5, remaining above the eligibility value.

Both skin dose distributions satisfied the skin critical volume criterion (V_{23Gy} < 10 cc). Doses for the remaining organs at risk

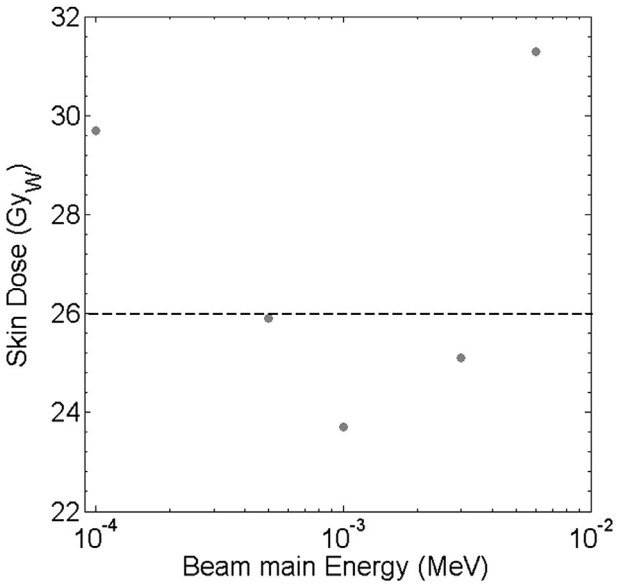

Figure 5. Maximum dose delivered in the skin as a function of the semi-ideal beam energy for case 1, when the treatment is optimized to obtain a 30 GyW PTV minimum dose. The dashed horizontal line represents the maximum tolerable dose for skin.

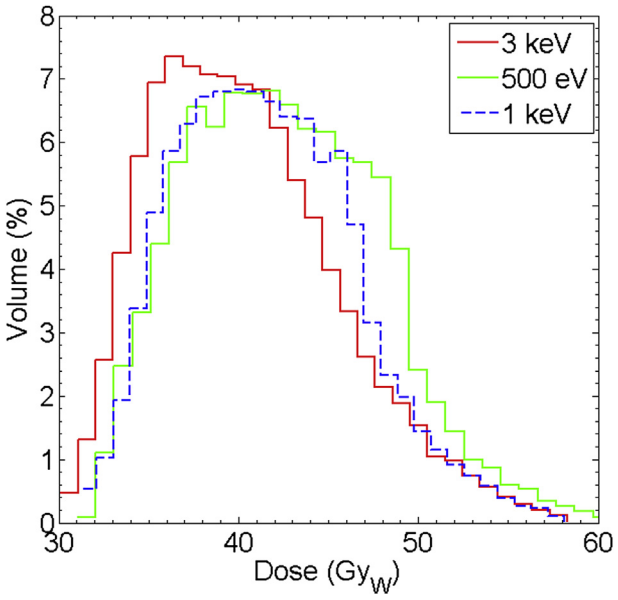

Figure 6. Differential dose volume histograms for the PTV of case 1, when semi-ideal 500 eV, 1 keV and 3 keV main energy beams are used with a 30 GyW minimum PTV dose prescription.

were far below constraints, with a reduction proportional to the updated PTV minimum dose.

Differential dose distributions for the PTV are presented in Fig. 7, where a comparison is shown between realistic beams and the best theoretical beam. The 1 keV beam proved the most suitable considering homogeneity and TCP in the PTV together with the minimum doses to the lung and skin. Note that although PTV doses are smaller in the case of realistic beams, TCPs values are still very high, with values of 0.77 and 0.81 for MIT-SPECT and CNEA-MEC beams, respectively.

Case 2: deep-seated localized NSCLC

The second clinical case considered is a patient with an NSCLC (T1N0M0) treated by fractionated 3DC-RT.

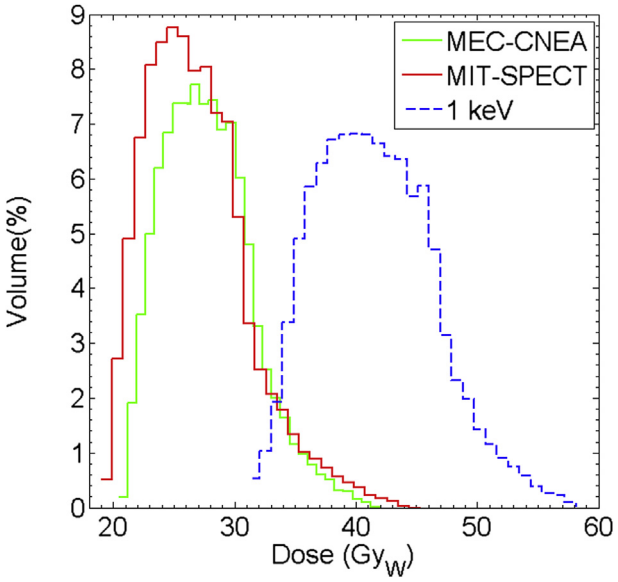

Figure 7. Differential dose volume histograms for the PTV of case 1 when MIT-SPECT and CNEA-MEC beams are used. Best semi-ideal beam distribution is presented.

A small CTV (2.5 cc) was contoured in the middle upper right lung. In order to assure complete target coverage during normal breath motion, PTV contouring was performed following clinical criteria, increasing CTV 30 mm in all directions resulting in a ~35 times increment in PTV volume.

Six beams distributed around the PTV isocenter point were tested for this case, as shown in Fig. 8. For all the semi-ideal neutron beams the configuration composed by posterior, left oblique anterior, and right oblique anterior incidences proved to be the best. However, for realistic beams, a fourth portal was added (Right Posterior Oblique) to obtain a suitable treatment.

Partial results of case 2. The 1 keV semi-ideal beam ensured the best dosimetric results. The spinal cord received the highest dose if compared to the constraints, the absorbed dose being however 25% lower than tolerance. The healthy lung volumes receiving less than 7 Gy$_W$ and 7.4 Gy$_W$ are 1200 cc and 1240 cc, respectively. Even these values were within the 20% probability of pneumonitis constraint, the 30 Gy$_W$ in the PTV could not be reached without exceeding maximum dose in the skin (the excess is almost 4 Gy$_W$). Then, the PTV minimum dose was maximized without over exceeding safety dose levels. Time windows optimization algorithm was applied in order to maximize the ratio between mean healthy lung dose and the PTV minimum dose resulting in an irradiation start time 5 h after infusion, with a 90 min duration. Values for the mean boron concentration in blood (~11 ppm) and the tumour to blood ratio (~2.5) lie again in the potential therapeutic range. While the PTV minimum dose was reduced to 20 Gy$_W$, the TCP value is still high about 0.8.

Healthy lung volumes receiving less than 7 Gy$_W$ and 7.4 Gy$_W$ are 1500 cc and 1517 cc, respectively, fulfilling the most conservative dose constraints.

When realistic beams were used with the 30 Gy$_W$ prescription to the PTV, skin maximum doses and V_{23} were over the recommended constraints. Then, the second optimization criterion for establishing a suitable treatment was applied.

Both beams accomplished the best dosimetry with the 4-portal configuration described in Fig. 8. Irradiation times were around 70 min, 20% shorter than the total time for the 1 keV ideal beam. No significant differences between treatments starts were found for the different beams. Mean tumour boron concentration was 2.3

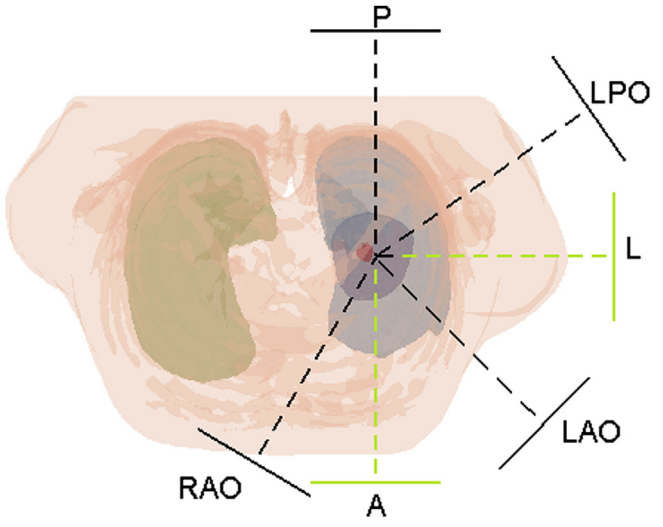

Figure 8. Patient 3D reconstruction. Complete set of portal incidences tested in case 2 distributed around PTV isocenter point. Highlighted darker dashed lines are those portals corresponding to the best configuration obtained.

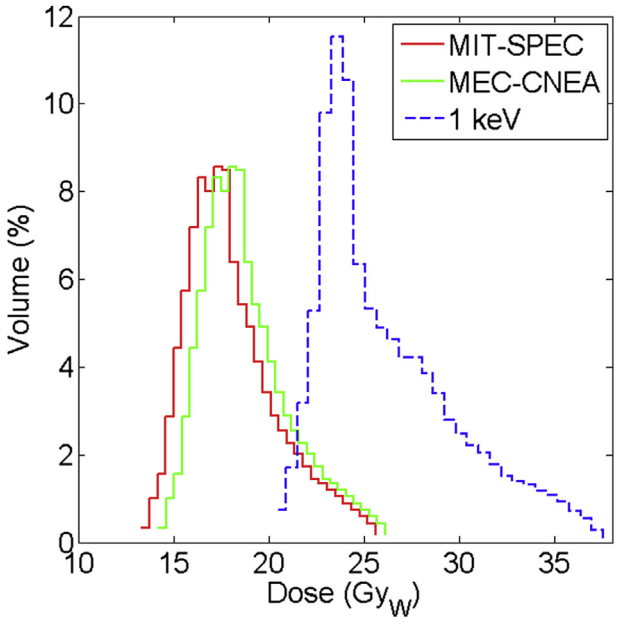

Figure 9. Differential dose volume histogram for the PTV when the realistic epithermal neutron beams (MIT-SPECT & MEC-CNEA) are used in case 2 compared with the best obtained semi-ideal 1 keV beam configuration.

times the value in healthy lung, ratio that, as previously mentioned, is considered suitable for patient eligibility in BNCT protocols.

For the mentioned treatment conditions, PTV minimum doses were around 13 Gy_W. Fig. 9 compares differential dose volume histograms obtained for the PTV using different beams. As expected for both realistic beams, mean and maximum doses are smaller than those for the 1 keV beam, but high enough to derive favourable TCP values, greater than 0.6.

Skin dose distributions satisfied the V_{23} constraint showing maximum values of 26 Gy_W, while healthy lung volumes receiving less than 7 Gy_W are all within the constraint value.

For this case, reducing the number of beam incidences to less than 3 (or 4, according to the particle source) resulted in skin doses over 30 Gy_W. Moreover, if one of these portals was a direct posterior field, the spinal cord dose was dangerously close to the constraint. On the other hand, when the number of portals was increased to 5 (or 6), the skin dose exceeded the constraints and therapeutic advantages in the healthy lung decreased.

Evaluation of conformity index (CI) parameter for localized NSCLC

For cases 1 and 2, CIs and LCIs for 80%, 60% and 40% isodoses were computed and compared with the intervals reported by Ong et al. [25].

As expected, when entire thorax isodoses are computed, the resulting CIs for BNCT tend to be over the corresponding SABR intervals. This is associated to the unavoidable background dose in the soft tissue and bones not due to the boron component. Nevertheless, the doses received by these tissues are well below the safety constraint values. Regarding LCIs, all BNCT values are inside or even below the statistical Ong's values showing clearly the steep falloff obtained from boron biological selectivity.

Oligometastatic disease

The third case studied is a theoretical oligometastatic NSCLC with absence of extra-thoracic disease, for which surgery is not possible and only systemic therapy is recommended. Under these conditions, BNCT can be proposed on the assumption that combining biological targeting and high LET radiation would favour the treatment of delocalized cancer, such as micrometastatic or diffuse disease.

Given that the location of the lesions was considered unknown, a four portal configuration, with beams of 20 cm diameter was proposed in order to provide full lung volume coverage, as shown in Fig. 10. Beam incidences were set with an oblique orientation towards patient isocenter point, defined as the midpoint between lungs in all directions (Fig. 10b).

The algorithm for optimizing the treatment time window was applied in order to maximize the difference between the healthy lung mean dose (7.5 Gy_W) and the PTV minimum dose, without exceeding the normal tissue constraints. Treatment starts 6–7 h after the end of boron infusion were obtained, with a total duration from 92 to 98 min. Blood boron concentration values averaged over the treatment time windows ranged from 7.7 to 9.7 ppm with associated tumour-to-blood ratios of 3.2 to 2.7.

Doses for all OARs excluding healthy lung were far below the corresponding constraints in all cases. Minimum doses delivered to the PTV were ~8.3 Gy_W, while mean and maximum doses reached values of ~20 Gy_W and~26 Gy_W, respectively (Fig. 11).

The dose analysis in the lung volume shows the biological selectivity of BNCT: when the same volume is exposed to the neutron irradiation, different doses are absorbed according to

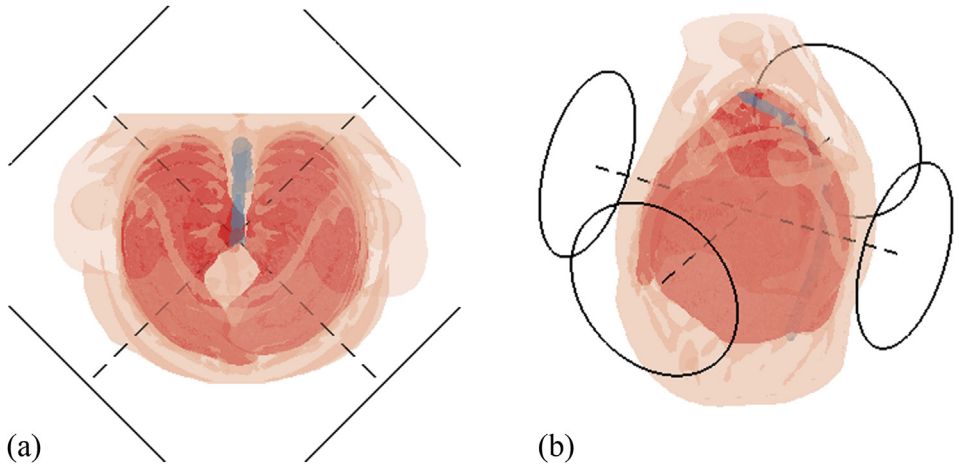

Figure 10. (a) Upper view of patient with the 4-portal configuration centred in the isocenter point. (b) 3D patient view showing the portal configuration in perspective. Lung volume is depicted in red. (For interpretation of the references to colour in this figure legend, the reader is referred to the web version of this article.)

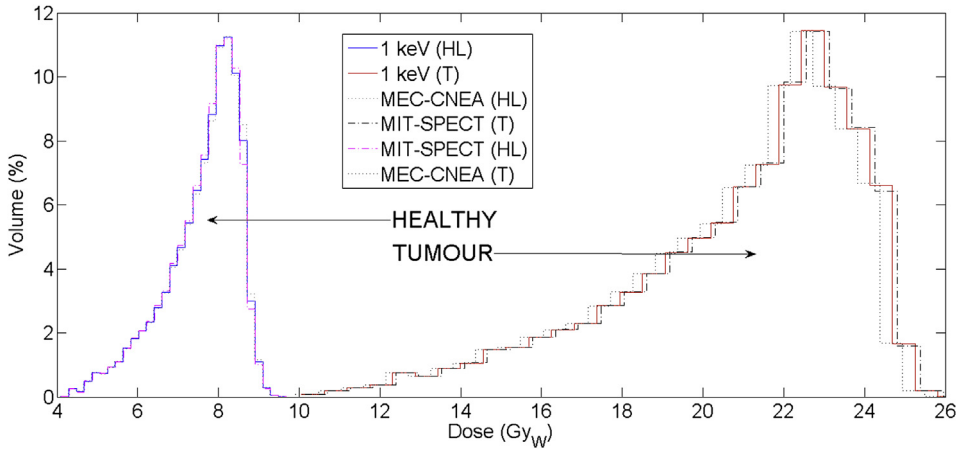

Figure 11. Differential dose volume histograms obtained for lung with a suitable portal configuration using a semi-ideal 1 keV centred beam and realistic beams (MIT-SPECT MEC-CNEA), considering the whole volume as healthy lung (HL) or as tumour (T). BNCT biological selectivity effect is observed in the resulting doses. Healthy lung doses are on the left side while tumour locate in the right side of the figure.

boron concentration. Maximum dose in healthy lung is in all cases lower than the minimum dose if it were tumour tissue.

To consider a realistic clinical scenario, five spherical lesions were randomly generated inside the lung volume with sizes uniformly sampled between 0.2 cc and 19 cc, with a mean of 3.3 cc [28]. This procedure was repeated 2000 times to explore the whole lung. For each trial, the expected number of controlled lesions was computed. The cumulative probability distribution is plotted in Fig. 12, showing that in 93% of the cases, the expected number of controlled lesions is 50% (2.5 nodules) or more. Moreover, the average of these expected numbers is 3.02 ± 0.04. This results shows that, although a generic total lung irradiation configuration is applied because the specific location of the lesions is unknown, there are good chances that most of the lesions are controlled.

Discussion and conclusion

One novel element introduced in this work is the possibility to fix the start time and the duration of the irradiation according to the information of normal and tumour boron concentration–time profiles for lung, derived from pre-clinical studies. In all studied scenarios, the time elapsed between BPA infusion and neutron irradiation resulted longer than the one adopted in clinical BPA-based treatments. On the other hand, treatment times are within classical values. Average tumour-to-normal tissue ratios derived from boron profiles (from 2.3 to 3.2) satisfy the patient eligibility criteria in BNCT protocols and lie in the range considered useful for effective treatments. These values, although similar to those observed in clinic, are below the 3.5 value usually applied for feasibility assessment of BNCT from a viewpoint of dose distribution analysis. Thus, the analysis presented in this work is conservative as concerns the boron concentration ratios, the results being even superior if the 3.5 tumour-to-healthy lung relationship is applied.

Another important result is that energies between 500 eV and 3 keV allow favourable dose distributions and high TCPs when suitable multiple portal treatments are designed. This differs from what stated in several BNCT publications stating that the treatment of deep-seated tumours requires neutron energies of the order of 10 keV. Energies outside the range [500 eV–3 keV] fail to deliver a potentially therapeutic dose to the tumour without exceeding the safety doses of the OARs. Particularly, skin ulceration and ribs fracture dose limits restrict the treatment duration and reduce the dose delivered to tumour.

Two realistic beams not specifically tailored for thorax irradiation were tested and proved suitable for delivering potential therapeutic doses. The best dosimetric performance was shown by MEC-CNEA beam that has a greater percentage of neutron contribution in the optimal range. The favourable obtained results support the hypothesis that it is possible to treat lung tumours that today have limited options due to their location or dissemination especially if a tailored beam is available.

Designed treatment plans confirmed the idea that multiple portal irradiation improves BNCT dose homogeneity in thorax tumours [3]. However, due to the boron washout as a function of time, and the fact that the patient has to be re-positioned for each field, special attention must be paid in order to perform optimal and realizable plans according to the available treatment facility. Dose overlapping around source edges may result in unacceptable values, especially for superficial OARs that play an important role regarding dose constraints. In this work, an angular separation between beams central axis higher than 40° proved suitable for localized tumour cases, with plans comprising 3 to 4 portals with

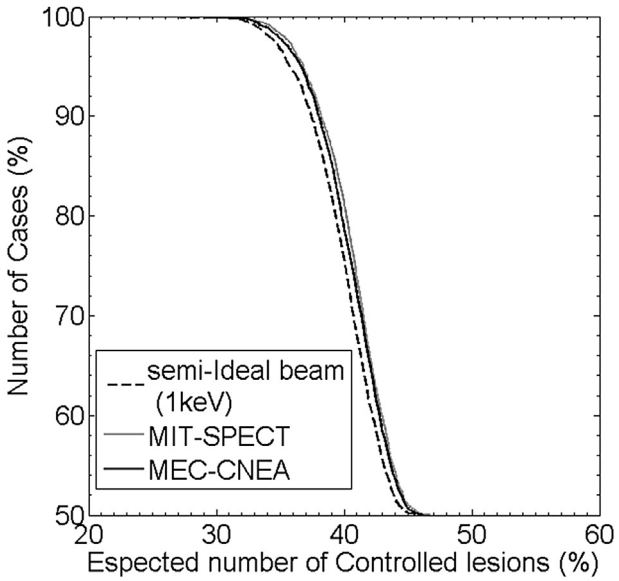

Figure 12. Cumulative probability distributions of the expected number of controlled lesions (%), obtained for 5 tumour lesions distributed randomly in the lung volume with the semi-ideal 1 keV centred beam (dash line), and the realistic-epithermal neutron beams MIT-SPECT (gray) and CNEA-MEC (black).

10–20 cm beam diameters. Beam incidences should be kept in the same plane (i.e., single arc) in order to reduce positioning uncertainties and dead time for repositioning.

In order to evaluate the effectiveness of NSCLC BNCT, a TCP based on the Hug-Kellerer survival model was introduced and validated. This sensitive figure of merit serves as a practical measure of the impact that the chosen parameters may have in the analysed treatments. As an example, in the oligometastatic case the TCP was 0.6 using a tumour-to-normal lung boron concentration ratio of 2.9, but applying the usual value of 3.5 adopted in clinic, the TCP becomes 0.8. Furthermore, given that HK model proved suitable to predict the effect for high-dose ablative radiotherapy, the presented TCP could be straightforwardly applied also to SABR.

For both localized NSCLC cases, the treatments plans employing 1 keV neutron beam achieved TCP values of ~0.8 or higher, even without imposing the minimum tumour dose to be as high as 30 Gy (SABR single fraction minimum prescription dose). With the realistic beams, the TCP values are also promising. Suzuki et al. [3] pointed out that shallow recurrent tumours in the chest wall or on the pleura are good candidates for BNCT, and this is in fact confirmed by the results obtained in case 1 that shows the most favourable TCP. In addition, our findings show that even without considering specific designed beams for thorax BNCT, an adequate dose can be delivered also to deep-seated lesions resulting in advantageous tumour control values.

For the theoretical case of oligometastatic disease, a mean number of expected controlled lesions as high as 60% was obtained. Even though this is not a common approach in clinic, where the irradiation is often delivered to a restricted lung volume, whole lung irradiation for tumour spreads in cases of Wilms or Ewing metastases has been performed with promising results. Recent publications on these cases present good overall survival (OS) when irradiation is offered as a concomitant treatment [29]. The observed lung toxicity, that represents the main concern when whole organ irradiation is conceived, is also acceptable. The proposed BNCT course takes only one session to deliver similar or even higher doses to the tumour than a traditional fractionated radiation protocol resulting in at least the same OS; moreover, given the biological selectivity, it would also ensure a significantly lower toxicity.

In conclusion, the presented lung tumour cases having poor therapeutic options with other forms of radiotherapies due to their locations, stage or overall patient status would definitively benefit from BNCT.

Acknowledgements

The authors gratefully acknowledge the continuous technical and scientific support of the CNEA and Pavia BNCT staffs. This work has been partially funded by INFN, section of Pavia.

Appendix A. A suitable TCP model for NSCLC

Martel et al. [20] have estimated the parameters of a tumour control probability model for non-uniform dose distributions from a retrospective analysis of 66 patients of NSCLC treated with photon radiation therapy in 1.8–2.0 Gy fractions and curative intent. Assuming that the tumour volume is composed of fractional volumes v_i each receiving uniform dose D_i, and that each v_i has an independent radiosensitivity, they proposed that the TCP_{total} of an inhomogeneously irradiated tumour can be expressed as.

$$TCP_{total} = \prod_i [TCP(D_i, 1)]^{v_i}, \tag{A1}$$

where $TCP(D_i, 1)$ is the dose–response function for the entire volume applied to each v_i with $D = D_i$. The expression for the TCP in Martel's work was the logistic function that models the binary dose response of a uniformly irradiated tumour

$$TCP(D) = \frac{1}{1 + \left(\frac{D_{50}}{D}\right)^{4\gamma}}, \tag{A2}$$

with D_{50} the dose needed to achieve the 50% of tumour control, and γ the normalized slope of the sigmoid shaped dose–response curve at D_{50}.

Table 2 summarizes the parameters D_{50} and γ estimated from the clinically observed local progression-free survival (LPFS) at three time intervals from Kaplan–Mayer plots.

Table 2
Martel et al. [20] estimations for dose and γ at 50% LPFS, considering patients of NSCLC treated with daily fraction sizes of 1.8–2.0 Gy.

	Time interval (months)		
	12	24	30
Dose at 50% LPFS (Gy)	64.0 ± 7.0	72.0 ± 2.5	84.5 ± 8.0
γ at 50% LPFS (range)	1.3 (0.9–3)	2.0 (1–4)	1.5 (0.8–3)

In order to use Eq. (A1) and Martel's estimates listed in Table 2 for computing TCPs in BNCT, it is necessary to adequately convert the large single radiation doses delivered per treatment to those equivalents for a 2 Gy/fraction scheme.

The survival dose–response relationship is assumed to be correctly described by the Hug-Kellerer survival model (HK).

$$S_{HK}(D) = exp\left(-k_1 D + k_2\left(1 - e^{-k_3 D}\right)\right), \tag{A3}$$

with $k_i, i = 1, \cdots, 3$, adjustable parameters.

González & Santa Cruz [30] (App. III, A10) have shown that the Hug-Kellerer survival model for a multifraction regime of dose delivery is.

$$S_{HK}(D, d) = \exp\left(-Dk_1 - \frac{k_2\left(1 - e^{-k_3 d}\right)}{d}\right), \tag{A4}$$

where D is the total dose given in n fractions, and d the dose per fraction ($D = nd$. Following Eq. (A3), the total biological effect E_n for a series of n fractions of size d is

$$E_n(D, d) = D\left(k_1 - k_2\left(1 - e^{-k_3 d}\right)/d\right). \tag{A5}$$

If E_{1i} is the biological effect for each fractional volume v_i that received one dose fraction of d_i ($E_{1i} = k_1 d_i - k_2(1 - e^{-k_3 d_i})$), then D_i is found from.

$$E_n(D_i, 2Gy) = E_{1i}. \tag{A6}$$

Solving Eq. (A5) for D_i the total equivalent dose for a 2 Gy/fraction scheme in expression (A1) is.

$$D_i = \frac{E_{1i}}{\left(k_1 - k_2\left(1 - e^{-k_3 2Gy}\right)/2Gy\right)}. \tag{A7}$$

The parameters of the Hug-Kellerer survival model were inferred by means of a least-square minimization method using the high-dose survival curve of the H460 non-small lung cancer cell line reported by Park et al. [31].[2] HK model provides an excellent fit

[2] Parameters with 95% confidence bounds: $k_1 = 1.81(1.79, 1.83)$,$k_2 = 15.42$ $(1494, 15.90)$ and $k_3 = 0.118(0.111, 0.126)$.

Table 3
Clinical results obtained with SBRT for definitive radiation of stage I NSCLC and predicted tumour control.

Series	Dose per fraction	No. of fractions	Prescription point	Derived max./min dose in the PTV	Observed tumour control[a]	Predicted tumour control[b]
Fritz 2006 [32]	30	1	80% isodose at PTV periphery	30.00/24.00	80.0%	82.5%
Baumann 2009 [34]	15	3	67% isoline at PTV periphery	22.00/14.75	93.0%	95.6%
Ricardi 2010 [35]	15	3	80% isodose- encompassing PTV to 100% at isocenter	18.75/15.00	92.7%	94.5%
Takeda 2009 [31]	10	5	80% isodose at PTV periphery	12.50/10.00	95.2%	92.0%

[a] At least 2-year crude tumour control data.
[b] Predicted values based on Eq. (A5) with D_{50} and γ from Park et al. for 30 months.

over the entire dose range of the data, and thus proves suitable to predict the effect for high-dose ablative radiotherapy.

Based on Eq. (A1) with D_i given in (A5) and the estimates of the HK model adjustable parameters $k_i, i = 1, \cdots, 3$, the predictive power of the proposed TCP model is evaluated using the data of stage I NSCLC patients treated with different fractionation schemes of definitive SABR.

Table 3 summarizes the clinical results obtained by different groups including studies of SABR with at least 2-year crude tumour control data [32,33]. The data comprise tumour control together with the dose per fraction, the number of fractions, the prescription point and the dose per fraction corrected at isocenter. From these data, the maximum and minimum dose in the PTV were derived. Assuming that doses in the PTV are distributed following a truncated Gaussian distribution between the derived minimum and maximum dose, the predicted tumour control for each clinical study can be calculated. The parameters D_{50} and γ used in the *TCP* model correspond to those obtained by Park et al. [31] for 30 months (see Table 2). As shown in Table 3, the predicted tumour control matches perfectly the clinical outcome for all analysed fractionation schemes (No of fractions ranging from 1 to 5), and therefore the proposed TCP model is considered suitable also for predicting tumour control in the BNCT scenario.

References

[1] Barth RF, Coderre JA, Vicente MGH, Blue TE. Boron neutron capture therapy of cancer: current status and future prospects. Clin Cancer Res 2005;11:3987–4002.
[2] Kiger JL, Kiger WS, Patel H, Binns PJ, Riley KJ, Hopewell JW, et al. Effects of boron neutron capture irradiation on the normal lung of rats. Appl Radiat Isot 2004;61:969–73.
[3] Suzuki M, Suzuki O, Sakurai Y, Tanaka H, Kondo N, Kinashi Y, et al. Reirradiation for locally recurrent lung cancer in the chest wall with boron neutron capture therapy (BNCT). Int Cancer Conf J 2012;1:235–8.
[4] Bortolussi S, Bakeine JG, Ballarini F, Bruschi P, Gadan MA, Protti N, et al. Boron uptake measurements in a rat model for boron neutron capture therapy of lung tumours. Appl Radiat Isot 2011;69:394–8.
[5] Trivillin VA, Garabalino MA, Colombo LL, González SJ, Farías RO, Monti Hughes A, et al. "Biodistribution of the boron carriers boronophenylalanine (BPA) and/or decahydrodecaborate (GB-10) for boron neutron capture therapy (BNCT) in an experimental model of lung metastases. Appl Radiat Isot 2014;88:94–8.
[6] X-5 Monte Carlo Team. MCNP — a general Monte Carlo n-particle transport code, version 5, Volume I: Overview and Theory, 3 vols. Los Alamos National Laboratory; 2003.
[7] International Commission on Radiological Units and Measurements. Nuclear data for neutron and proton radiotherapy and for radiation protection. ICRU Rep 2000:63.
[8] Herrera MS, González SJ, Minsky DM, Kreiner AJ. Evaluation of performance of an accelerator-based BNCT facility for the treatment of different tumor targets. Phys Med 2013;29:436–46.
[9] Kiger WS, Sakamoto S, Harling OK. Neutronic design of a fission converter-based epithermal neutron beam for neutron capture therapy. Nucl Sci Eng 1999;131:1–22.
[10] Capoulat ME, Minsky DM, Kreiner AJ. Computational assessment of deep-seated tumor treatment capability of the 9Be(d,n)10B reaction for accelerator-based Boron Neutron Capture Therapy (AB-BNCT). Phys Med 2014;30:133–46.
[11] Goorley JT, Kiger WS, Zamenhof RG. Reference dosimetry calculations for neutron capture therapy with comparison of analytical and voxel models. Med Phys 2002;29:145–56.
[12] N. US Department of Commerce, "NIST: X-Ray mass attenuation coefficients." [Online]. Available: http://www.nist.gov/pml/data/xraycoef/index.cfm. [accessed on 2.6.14].
[13] Nakagawa T, Shibata K, Chiba S, Fukahori T, Nakajima Y, Kikuchi Y, et al. Japanese evaluated nuclear data library version 3 Revision-2: JENDL-3.2. J Nucl Sci Technol 1995;32:1259–71.
[14] Kiger JL, Kiger WS, Riley KJ, Binns PJ, Patel H, Hopewell JW, et al. Functional and histological changes in rat lung after Boron Neutron Capture Therapy. Radiat Res 2008;170:60–9.
[15] González SJ, Bonomi MR, Santa Cruz GA, Blaumann HR, Larrieu OAC, Menéndez P, et al. First BNCT treatment of a skin melanoma in Argentina: dosimetric analysis and clinical outcome. Appl Radiat Isot 2004;61:1101–5.
[16] Coderre JA, Morris GM. The radiation biology of boron neutron capture therapy. Radiat Res 1999;151:1–18.
[17] Kiger WS, Palmer MR, Riley KJ, Zamenhof RG, Busse PM. A pharmacokinetic model for the concentration of 10B in blood after boronophenylalanine-fructose administration in humans. Radiat Res 2001;155:611–8.
[18] Suzuki M, Endo K, Satoh H, Sakurai Y, Kumada H, Kimura H, et al. A novel concept of treatment of diffuse or multiple pleural tumors by boron neutron capture therapy (BNCT). Radiother Oncol 2008;88:192–5.
[19] Suzuki M, Sakurai Y, Masunaga S, Kinashi Y, Nagata K, Maruhashi A, et al. Feasibility of boron neutron capture therapy (BNCT) for malignant pleural mesothelioma from a viewpoint of dose distribution analysis. Int J Radiat Oncol 2006;66:1584–9.
[20] Martel MK, Ten Haken RK, Hazuka MB, Kessler ML, Strawderman M, Turrisi AT, et al. Estimation of tumor control probability model parameters from 3-D dose distributions of non-small cell lung cancer patients. Lung Cancer 1999;24:31–7.
[21] Ettinger DS, Akerley W, Borghaei H, Chang AC, Cheney RT, Chirieac LR, et al. Non–Small cell lung Cancer, version 2.2013. J Natl Compr Canc Netw 2013;11(6):645–53.
[22] Timmerman R, Paulus R, Galvin J, Michalski J, Straube W, Bradley J, et al. Stereotactic body radiation therapy for inoperable early stage lung cancer. JAMA 2010;303(11):1070–6.
[23] Benedict SH, Yenice KM, Followill D, Galvin JM, Hinson W, Kavanagh B, et al. Stereotactic body radiation therapy: the report of AAPM Task Group 101. Med Phys 2010;37:4078–101.
[24] Fritz P, Kraus H-J, Blaschke T, Mühlnickel W, Strauch K, Engel-Riedel W, et al. Stereotactic, high single-dose irradiation of stage I non-small cell lung cancer (NSCLC) using four-dimensional CT scans for treatment planning. Lung Cancer 2008;60:193–9.
[25] Ong CL, Palma D, Verbakel WFAR, Slotman BJ, Senan S. Treatment of large stage I–II lung tumors using stereotactic body radiotherapy (SBRT): planning considerations and early toxicity. Radiother Oncol 2010;97:431–6.
[26] Hellman S, Weichselbaum RR. Oligometastases. J Clin Oncol 1995;13:8–10.
[27] Van Dyk J, Keane TJ, Kan S, Rider WD, Fryer CJH. Radiation pneumonitis following large single dose irradiation: a re-evaluation based on absolute dose to lung. Int J Radiat Oncol 1981;7:461–7.
[28] Ricardi U, Filippi AR, Guarneri A, Ragona R, Mantovani C, Giglioli F, et al. Stereotactic body radiation therapy for lung metastases. Lung Cancer 2012;75:77–81.
[29] Bölling DT, Schuck A, Paulussen M, Dirksen U, Ranft A, Könemann S, et al. Whole lung irradiation in patients with exclusively pulmonary metastases of Ewing tumors. Strahlenther Onkol 2008;184:193–7.
[30] González SJ, Cruz GAS. The photon-isoeffective dose in Boron neutron capture therapy. Radiat Res 2012;178:609–21.
[31] Park C, Papiez L, Zhang S, Story M, Timmerman RD. Universal survival curve and single fraction equivalent dose: useful tools in understanding potency of ablative radiotherapy. Int J Radiat Oncol 2008;70:847–52.
[32] Fritz P, Kraus H-J, Muhlnickel W, Hammer U, Dolken W, Engel-Riedel W, et al. Stereotactic, single-dose irradiation of stage I non-small cell lung cancer and lung metastases. Radiat Oncol 2006;1:1–9.
[33] Mehta V. Radiation pneumonitis and pulmonary fibrosis in non–small-cell lung cancer: pulmonary function, prediction, and prevention. Int J Radiat Oncol 2005;63:5–24.
[34] Baumann P, Nyman J, Hoyer M, Wennberg B, Gagliardi G, Lax I, et al. Outcome in a prospective phase II trial of medically inoperable stage I non–small-cell lung cancer patients treated with stereotactic body radiotherapy. J Clin Oncol 2009;27:3290–6.
[35] Ricardi U, Filippi AR, Guarneri A, Giglioli FR, Ciammella P, Franco P, et al. Stereotactic body radiation therapy for early stage non-small cell lung cancer: results of a prospective trial. Lung Cancer 2010;68:72–7.